

## Room-temperature AlInAs/InGaAs/InP quantum cascade lasers

Piotr Gutowski, Piotr Karbownik, Artur Trajnerowicz, Kamil Pierściński, Dorota Pierścińska, Iwona Sankowska, Justyna Kubacka-Traczyk, Maciej Sakowicz, Maciej Bugajski

*Institute of Electron Technology, Al. Lotników 32/46, 02-668 Warszawa*

Received November 24, 2014; accepted December 04, 2014; published December 31, 2014

**Abstract**—The room-temperature (300K), pulsed mode operation of InP-based quantum cascade laser (QCL) is reported. This has been achieved by the use of a lattice matched AlInAs/InGaAs/InP heterostructure. Its design follows a 4-well, 2-phonon resonance scheme. The QCL structures were grown by MBE in a Riber Compact 21T reactor. The lasers utilize an AlInAs waveguide and were grown exclusively by MBE without MOVPE regrowth. High operating temperatures have been achieved by careful optimization of growth and processing technology.

Coherent sources in the mid-IR spectral range are of great interest due to a large number of their applications in high-resolution molecular spectroscopy, industrial control and medical diagnostics. For the above reasons, over the last twenty years a big effort has been made to develop highly efficient quantum cascade lasers (QCLs) operating at this wavelength range.

In this paper we present the development of lattice matched ( $\sim 9.2\mu\text{m}$ )  $\text{Al}_{0.48}\text{In}_{0.52}\text{As}/\text{In}_{0.53}\text{Ga}_{0.47}\text{As}/\text{InP}$  QCLs technology. The laser structures consisted of 30-segments. The active region of the lasers was of 4-well 2-phonon resonance design [1]. The layer sequence of one period of the structure, in nanometers, starting from the injection barrier is: **4.0**, 1.9, **0.7**, 5.8, **0.9**, 5.7, **0.9**, 5.0, **2.2**, 3.4, **1.4**, 3.3, **1.3**, 3.2, 1.5, 3.1, **1.9**, 3.0, **2.3**, 2.9, **2.5**, **2.9** nm. The AlInAs layers are denoted in bold. The underlined layers are  $n$  doped to  $1.5 \times 10^{11}\text{cm}^{-2}$  or  $2.0 \times 10^{11}\text{cm}^{-2}$ . The conduction band profile and moduli squared wavefunctions in an injector/active/injector segment of the  $\text{Al}_{0.48}\text{In}_{0.52}\text{As}/\text{In}_{0.53}\text{Ga}_{0.47}\text{As}/\text{InP}$  laser under the applied field of 50 kV/cm are shown in Fig. 1. The electronic band structure of QCL has been calculated by solving the Schrödinger equation with a position dependent effective mass.

The waveguide from the bottom side was formed by a low doped InP substrate and from the top by a  $2.5\mu\text{m}$  AlInAs layer covered by a heavily doped InGaAs layer. The details of the layer structure of the investigated devices are listed in Table 1. The laser structures were grown exclusively by MBE without necessity of InP MOVPE regrowth. For epitaxial process control, high resolution X-ray diffraction (HR XRD) was used.

\* E-mail: gutowski@ite.waw.pl

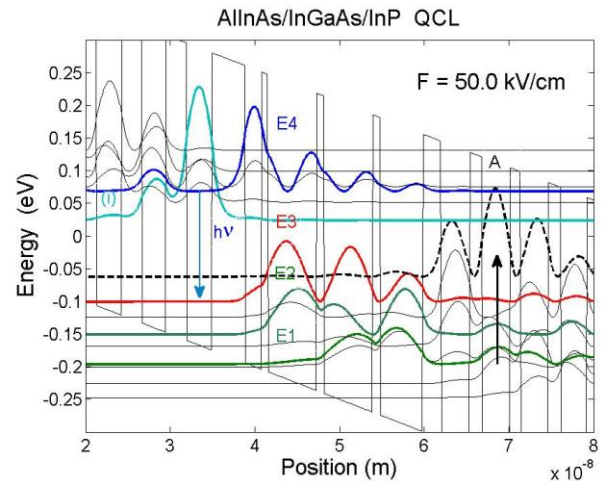


Fig. 1. Conduction band profile and moduli squared wavefunctions in an injector/active/injector segment of the laser under an applied field  $F=50\text{kV/cm}$  (at threshold). The wavefunctions have been shifted to energy positions of respective levels. E4, E3, E2 and E1 refer to the upper, lower and ground state of lasing transitions. The black dashed line denotes the "spurious" excited state in the injector minigap. The lowest energy state in the injector couples directly to the upper laser level E4.

Table 1. Layer structure of AlInAs/InGaAs/InP lasers.

500nm	InGaAs	$n=8e18\text{cm}^{-3}$	Upper Waveguide
$2.5\mu\text{m}$	AlInAs	$n=1e17\text{cm}^{-3}$	
500nm	InGaAs	$n=4e16\text{cm}^{-3}$	
$\sim 1.8\mu\text{m}$	<b>30 x AlInAs/InGaAs</b>		Active Region
500nm	InGaAs	$n=4e16\text{cm}^{-3}$	Lower Waveguide
500 $\mu\text{m}$ Substrate	InP	$n=2e17\text{cm}^{-3}$	

The XRD  $2\Theta/\omega$  scan of the QCL epitaxial structure is displayed in Fig.2. The period thickness determined by superlattice peaks spacing for the structures grown in the same campaign deviated less than 2% from the intended design. This growth accuracy guaranteed the lasing of all fabricated devices. The high crystal quality of the structures was additionally confirmed by reciprocal lattice mapping (Fig. 3) which shows negligible diffuse scattering and low residual mismatch strain.

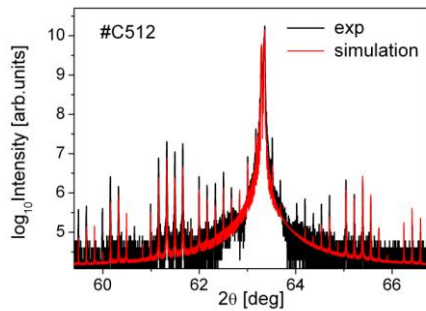


Fig. 2. Comparison of the experimental and simulated HRXRD  $2\theta/\omega$  profiles for the QCL structure. The period length and Al content in barriers are determined by fitting a simulated curve to an experimental one.

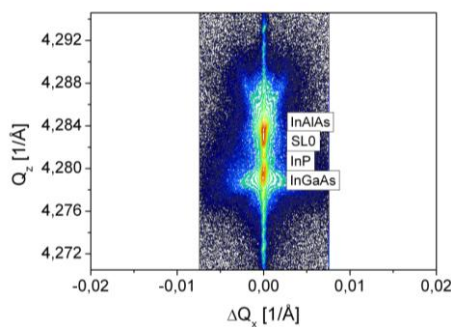


Fig. 3. Reciprocal lattice map of an  $\text{Al}_{0.48}\text{In}_{0.52}\text{As}/\text{In}_{0.53}\text{Ga}_{0.47}\text{As}/\text{InP}$  QCL structure.

The fundamental TM mode profile in the structure is shown in Fig. 4. The 2D waveguide analysis has been done by using a fully vectorial waveguide solver based on the film mode matching method [2].

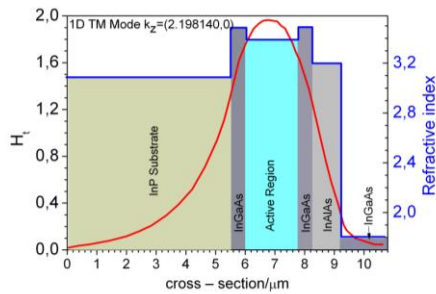


Fig. 4. The fundamental TM mode profile in the lattice matched an  $\text{Al}_{0.48}\text{In}_{0.52}\text{As}/\text{In}_{0.53}\text{Ga}_{0.47}\text{As}/\text{InP}$  laser.

The double trench lasers were fabricated using standard processing technology, i.e., wet etching and  $\text{Si}_3\text{N}_4$  for electrical insulation. Low resistivity, RTA alloyed at  $370^\circ\text{C}$  for 60s, Ti/Au ohmic contacts to epi-side and AuGe/Ni/Au at the substrate side of the device were used. For current injection,  $15\mu\text{m}$  and  $25\mu\text{m}$  wide windows were opened through the insulator. The lasers were cleaved to bars 1mm and 3mm long and soldered epi-side down to Au-plated copper mounts. We have used an indium soldering or direct Au/Au bonding. A device

mounting technique has been optimized for efficient heat management [3].

The room-temperature light-current and current-voltage characteristics of the laser are shown in Fig. 5. The threshold current density at the room temperature  $J_{\text{th}}$  is  $\sim 5\text{ kA}/\text{cm}^2$ , which is roughly 3 times lower than in the case of AlGaAs/GaAs lasers emitting at the same wavelength.

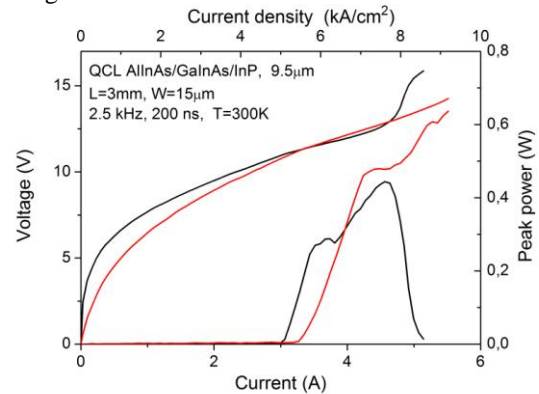


Fig. 5. Light-current and current-voltage characteristics of the  $\text{Al}_{0.48}\text{In}_{0.52}\text{As}/\text{In}_{0.53}\text{Ga}_{0.47}\text{As}/\text{InP}$  ( $\lambda=9.5\mu\text{m}$ ) laser driven by 200ns pulses with repetition rate of 2.5kHz.

Figure 5 shows L-I-V characteristics for two injector doping values. For lower doping ( $1.5 \times 10^{11}\text{ cm}^{-2}$ ) we observe power rollover due to level misalignment with a current increase. For higher doping the dynamic range of operation extends and higher powers can be obtained before either pure Stark or thermal rollover [4]. However, the penalty for higher power is an increase in threshold current density of the laser. To lower the absolute threshold current, one can use a shorter cavity. This is illustrated in Fig. 6, which shows the characteristics of a 1mm laser exhibiting the threshold  $< 1\text{ A}$ . Despite the small volume of active region, due to a relatively low amount of heat which has to be dissipated, the laser is able to emit comparable powers to 3 mm cavity lasers.

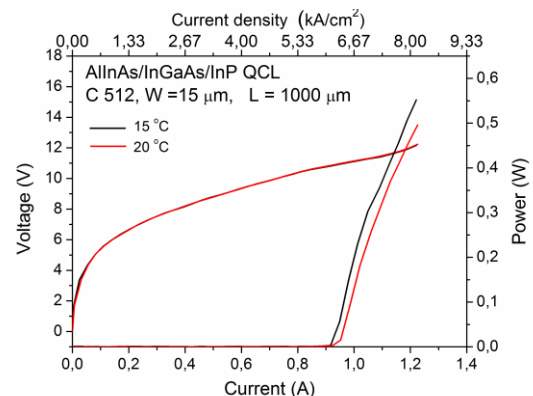


Fig. 6. Light-current and current-voltage characteristics of the  $\text{Al}_{0.48}\text{In}_{0.52}\text{As}/\text{In}_{0.53}\text{Ga}_{0.47}\text{As}/\text{InP}$  ( $\lambda=9.2\mu\text{m}$ ) laser driven by 200ns pulses with a repetition rate of 1kHz.

The lasers worked up to 340K (~60°C) emitting tens of mW of pulse power. At 20°C the optical power per uncoated facet was of the order of 0.6W. The slope efficiency was up to 1W/A at room temperature; the wall plug efficiency was ~4%. The waveguide losses estimated by measuring devices with different resonator lengths, fabricated from the same epitaxial wafer are of the order of 18cm<sup>-1</sup>. This value can be further improved by optimizing the waveguide design, i.e., by employing a symmetric InP waveguide. In this case a conductive substrate can be used to grow a lower waveguide by MOVPE, then an active region is grown by MBE and finally the upper waveguide is completed by MOVPE. That complicates technology, although the clear advantage, despite the increase of a confinement factor, is the suppression of free carrier absorption in the lower waveguide.

The threshold current density can be calculated from the equation [5]:

$$J_{th} = \frac{1}{\tau_{eff}} \frac{\epsilon_0 n \lambda L_p \gamma_{43}}{4\pi e \Gamma |z_{43}|^2} (\alpha_w + \alpha_m), \quad (3)$$

where the effective lifetime  $\tau_{eff} = \tau_4 (1 - \tau_3/\tau_{43})$ . In this equation,  $\epsilon_0$  is the vacuum permittivity,  $n$  is the effective refractive index of the laser mode,  $\lambda$  is the emission wavelength,  $L_p$  is the length of one period,  $\gamma_{43}$  is the full width at the half maximum (FWHM) of a spontaneous emission spectrum,  $e$  is the electron charge,  $\Gamma$  is the active region confinement factor and  $z_{43}$  is the matrix element of laser transition. The scattering times  $\tau_{ij}$  from the states  $i$  to  $j$  are dominated by LO-phonon emission. The mirror losses  $\alpha_m = \alpha_{m,c} = \ln(R)/2L$ , where  $R=0.297$  is the uncoated mirror reflectivity. Taking experimentally determined waveguide losses  $\alpha_w$  equal to 18cm<sup>-1</sup>, the confinement factor  $\Gamma=0.56$  and the effective refractive index  $n=3.4$  as well as  $\lambda=9.2\mu\text{m}$ ,  $\tau_{eff}=2.1\text{ps}$ ,  $\gamma_{43}=16\text{meV}$  and  $z_{43}=2.37\text{nm}$  we get  $J_{th}$  for the 3-mm-long device equal to  $\approx 3.5\text{kA/cm}^2$ , which is basically what we observe experimentally. The possible reason for high internal losses is not optimized injector doping.

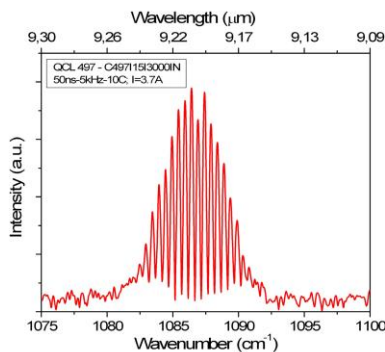


Fig. 7. Room temperature emission spectrum of Fabry-Perot (FP) laser ( $W=15\mu\text{m}$ ,  $L=3\text{mm}$ ) at  $I=1.15J_{th}$ .

The room temperature (RT) spectrum of an Al<sub>0.48</sub>In<sub>0.52</sub>As/In<sub>0.53</sub>Ga<sub>0.47</sub>As/InP laser driven by 50ns pulses with a repetition rate of 5kHz is shown in Fig.7. The spectrum shows a number of longitudinal modes, belonging to fundamental transverse mode, with spacing of  $\sim 0.44\text{cm}^{-1}$ , determined by the length of the resonator.

In conclusion, we have demonstrated the room temperature (P~0.6W) pulsed operation of an AlInAs/InGaAs/InP mid-infrared (~9.2μm) laser. This has been achieved by careful optimization of the epitaxial process and device fabrication technology. The parameters of developed devices are summarized in Table 2.

Table 2. Basic parameters of AlInAs/InGaAs/InP lasers.

Parameter	Symbol	Value
Threshold current density	$J_{th}$ (77 K)	2 kA/cm <sup>2</sup> – 3 kA/cm <sup>2</sup>
	$J_{th}$ (300 K)	~5 kA/cm <sup>2</sup>
Threshold voltage	$V_{th}$ (77 K)	10 V
	$V_{th}$ (300 K)	11 V
Peak power (per facet)	P (77 K)	~2 W
	P (300 K)	~0.6 W
Max operating T	$T_{max}$	340 K
Characteristic T	$T_0$ (K)	120 K-140 K
Differential gain	$g\Gamma$ (77K)	(5.7–6) cm <sup>-1</sup> /kA
	$g\Gamma$ (250K)	(1.9 - 2.5) cm <sup>-1</sup> /kA
Waveguide losses	$\alpha_w$ (77–300) K	~18 cm <sup>-1</sup>
Wall-Plug efficiency	WPE	~ 4 %
Slope efficiency	$\eta_{ext}$	~ 1 W/A

The 9.2μm - AlInAs/InGaAs/InP lasers utilize an AlInAs waveguide and were grown exclusively by MBE without MOVPE regrowth. They have the state-of-the-art parameters for this type of design.

This work was financially supported by the National Center for Research and Development (Poland) grant no. PBS 1/B3/2/2012 (EDEN) and grant no. PBS 2/A3/15/2013 (PROFIT). This publication has been co-financed with European Union funds by the European Social Fund.

## References

- [1] M. Beck, D. Hofstetter, T. Allen, J. Faist, U. Oesterle, M. Illegems, E. Gini, H. Melchior, *Science* **295**, 301 (2002).
- [2] FIMMWAVE ver. 5.3.9, Photon Design, [www.photon.com](http://www.photon.com).
- [3] K. Pierściński, D. Pierścińska, M. Iwińska, K. Kosiel, A. Szerling, P. Karbownik, and M. Bugajski, *J. Appl. Phys.* **112**, 043112 (2012).
- [4] M. Bugajski, K. Kosiel, A. Szerling, P. Karbownik, K. Pierściński, D. Pierścińska, G. Haldaś and A. Kolek, *Proc. SPIE* **8432**, 843201 (2012).
- [5] J. Faist, *Quantum Cascade Lasers* (Oxford University Press, Oxford 2013).